Available online at www.sciencedirect.com

ScienceDirect

Scripta Materialia 75 (2014) 26–29

Scripta MATERIALIA

www.elsevier.com/locate/scriptamat

Large magnetic entropy change and enhanced mechanical properties of Ni–Mn–Sn–C alloys

Yu Zhang,[a] Jian Liu,[a] Qiang Zheng,[b,c] Jian Zhang,[a] Weixing Xia,[a] Juan Du[a,*] and Aru Yan[a]

[a]*Key Laboratory of Magnetic Materials and Devices, Ningbo Institute of Material Technology and Engineering, Chinese Academy of Sciences, 519 Zhuangshi Road, Ningbo 315201, People's Republic of China*

[b]*School of Materials Science and Engineering, Ningbo University of Technology, Ningbo 315016, People's Republic of China*

[c]*Ningbo Branch of China Academy of Ordnance Science, Ningbo 315103, People's Republic of China*

Received 19 August 2013; revised 7 November 2013; accepted 8 November 2013
Available online 21 November 2013

The microstructure, magnetocaloric effect and mechanical properties of carbon-doped $Ni_{43}Mn_{46}Sn_{11}C_x$ ($x = 0$, 2, 4, 8) alloys have been investigated. The martensitic transformation temperatures increase remarkably, from 196 to 249 K, as the carbon doping content increases. A large magnetic entropy change, ΔS_M, from 27.4 J kg^{-1} K^{-1} with $x = 0$ to 34.6 J kg^{-1} K^{-1} with $x = 2$, was obtained for a field change of 5 T. A significant enhancement of compressive strength from 556 MPa with $x = 0$ up to 1016 MPa with $x = 8$ is ascribed to the appearance of high amount of carbides.

Keywords: Ni–Mn–Sn–C; Martensitic transformation; Microstructure; Magnetic entropy change; Compressive strength

Magnetic refrigeration based on the magnetocaloric effect (MCE) is potentially a high-efficiency, low-cost and greenhouse-gas-free refrigeration technology, which is drawing more attention as an alternative to the existing vapor compression refrigeration [1]. For a magnetic refrigeration material, a high magnetic entropy change, ΔS_M, is important for its application on the point of refrigeration capacity. In addition to magnetic properties, a magnetic refrigerant should have a certain degree of machinability in order to be fabricated into thin plates for the purpose of improving the heat-exchange performance [2]. Additionally, excellent mechanical properties guarantee a longer working life during magnetization–demagnetization cycles. Recently, magnetic refrigerants, such as Gd–Si–Ge [3], La–Fe–Si [4], Mn–Fe–P–As [5] and Ni–Mn-based Heusler alloys [6], have become the focus of research due to their giant MCE caused by first-order phase transition. Among them, the rare-earth-free Ni–Mn–X (X = Sn, In, Sb) Heusler alloy systems have provoked the greatest interest due to their large inverse MCEs [7–9].

To get a high ΔS_M and a suitable magnetic transition temperature (T_M), interstitial atoms such as B [10], H [11] and C [12] have been investigated with regard to their enhancement of MCE. Xuan et al. [10] studied the effect of interstitial B atom on the MCE of Ni–Mn–Sn alloys. The T_M could be changed markedly just by adjusting the amount of B, but the ΔS_M was also reduced significantly when doped with excessive B. Mandal et al. [11] studied the effect of interstitial H atoms on the MCE of La–Fe–Si alloys. Though the T_C could be changed markedly and the ΔS_M could not be changed much, the thermal stability of the hydride deteriated. Chen et al. [12] investigated the effect of interstitial C atom on the MCE of La–Fe–Si alloys. They found that a certain amount of C can adjust the Curie temperature of the alloy; at the same time, it did not reduce the ΔS_M substantially. So far, there have no reports on C doping in the Ni–Mn–Sn system, but it is expected that the ΔS_M would not change a lot.

There are many reports on adjusting the martensite transition temperature, enhancing the magnetic entropy change and reducing the hysteresis of the Ni–Mn–Sn alloy [13–16]. However, little research has been carried out on the machinability of the alloy, which is an additional property for a magnetic cooling device. Feng et al. [17] found that the mechanical properties of Ni–Mn–In alloys can be dramatically improved by adding Fe. It is thus possible to enhance the Ni–Mn-based alloys' mechanical

* Corresponding author. Tel.: +86 0574 86685150; e-mail: dujuan@nimte.ac.cn

1359-6462/$ - see front matter © 2013 Acta Materialia Inc. Published by Elsevier Ltd. All rights reserved.
http://dx.doi.org/10.1016/j.scriptamat.2013.11.009

strength when an ingredient with a high mechanical strength, such as a carbide, is added. Moreover, it is well known that carbides with high hardness and high melting point can enhance the mechanical properties of steel [18].

In this paper, C was introduced into Ni–Mn–Sn alloys with the expectation of gaining not only a relative high ΔS_M arising from the interstitial C atom, but also a relative high compressive strength due to the appearance of a second, carbide phase by appropriate adjustment of C content.

Ingots of $Ni_{43}Mn_{46}Sn_{11}C_x$ ($x = 0, 2, 4, 8$), denoted as C0, C2, C4 and C8, respectively, were prepared by arc-melting under a high-purity argon atmosphere. The purities of all of the raw elements are better than 99.9%. The ingots were homogenized by annealing in an evacuated sealed quartz tube at 1173 K for 24 h and then quenched in water. The crystal structure analyses were carried out by X-ray diffraction (XRD) using a Cu K_α radiation source at room temperature. The microstructure and composition were determined by scanning electron microscopy (SEM) using a JSM-6700F microscope equipped for energy-dispersive spectrometry (EDS). The magnetic measurements were carried out using a superconducting quantum interference device. The mechanical properties were ascertained using an Instron testing machine.

XRD patterns of the $Ni_{43}Mn_{46}Sn_{11}C_x$ ($x = 0, 2, 4, 8$) alloys are shown in Figure 1. All of the peaks correspond to the Heusler $L2_1$ cubic structure, which indicates that they are all austenitic phase and that the martensite transition temperature T_M is below room temperature. From the enlarged XRD pattern in the inset of Figure 1, all of the (220) peaks of samples C2–C8 are shifted towards lower angles compared to that of the C0 sample, which indicates an increase in lattice volume due to C atoms entering into the lattices. In contrast, compared with C2, the (220) peaks of C4 and C8 samples are shifted towards higher angles, indicating that the lattice volumes of C4 and C8 are smaller than that of C2. This may be caused by the change of Mn/Ni ratio induced by the second phase formed from C and manganese with increasing C content.

In fact, the second phase has already appeared from samples C2 to C8, as confirmed by the SEM images in Figure 2. The peaks of the second phase were not observed in the XRD pattern because of its low content except for C8, which has an extra peak corresponding to the carbide phase. Due to manganese loss induced by the second phase in the matrix phase, there is a shrink-

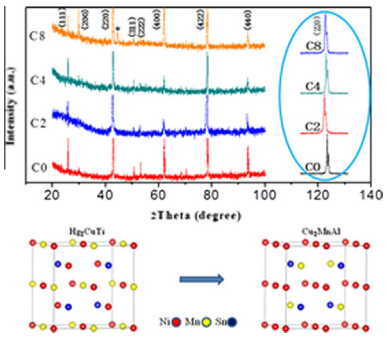

Figure 1. Top: XRD patterns of $Ni_{43}Mn_{46}Sn_{11}C_x$ ($x = 0, 2, 4, 8$) alloys at room temperature. The star symbol indicates manganese carbides. The enlarged (220) peak is presented in the inset. Bottom: the crystal structure change from Hg_2CuTi-type to Cu_2MnAl-type.

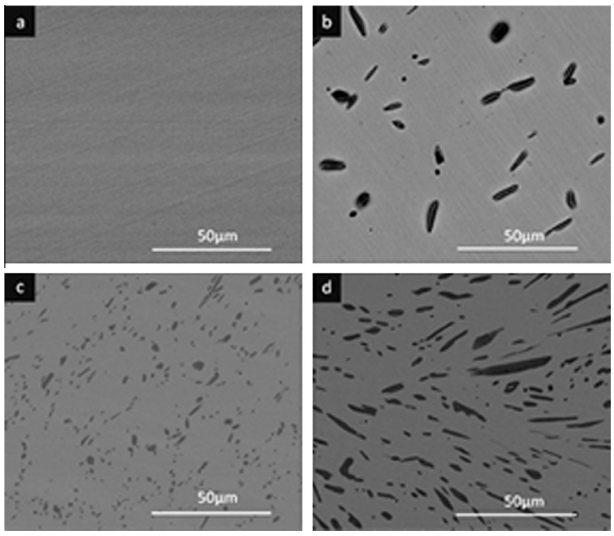

Figure 2. SEM images of $Ni_{43}Mn_{46}Sn_{11}C_x$ ($x = 0, 2, 4, 8$) alloys.

age in cell volume caused by the smaller atomic radius of nickel (1.25 Å) than that of manganese (1.79 Å). Subsequently, the XRD peaks of the C4 and C8 samples are shifted towards higher angles compared with that of C2. This is also confirmed by comparing the intensities of the (111) and (200) peaks. The higher intensity of the (111) peak compared to the (200) peak of samples C0, C2 and C4 indicates a highly ordered Hg_2CuTi-type structure [19]. The opposite result observed in C8 suggests that its crystal structure has changed to Cu_2MnAl-type. This change in crystal structure from Hg_2CuTi-type to Cu_2MnAl-type is shown in the lower part of Figure 1. The great loss of manganese from sample C8 results in a distortion of the crystal structure from the Hg_2CuTi-type to the Cu_2MnAl-type.

In order to confirm the existence of the second phase and the evolution of the composition with C doping, SEM was carried out on all of the samples, as shown in Figure 2. For $Ni_{43}Mn_{46}Sn_{11}$ without any C doping, there was only one uniform phase, as presented in Figure 2a. After C doping, a dark stripe-like second phase appears and its volume fraction increases with increasing C doping, as revealed in Figure 2b–d. EDS analysis showed that the second phase was manganese carbides.

The exact composition of the $L2_1$ phase was analyzed by EDS for all samples. The results are shown in Table 1. The interstitial C in the $L2_1$ phase increases slightly with increasing C doping. Except for the content entering interstitial positions, the excessive C would combine with the manganese to form islands of second phase beyond

Table 1. Compositions of the $L2_1$ phase for all samples determined by EDS analysis and the valence electron concentrations per atom, *e/a*, determined as the concentration-weighted sum of s, d and p electrons.

	Ni	Mn	Sn	C	*e/a*
C0	42.40	45.53	12.06		7.91
C2	42.33	45.05	11.90	2.71	7.92
C4	44.66	43.91	12.65	2.79	7.95
C8	48.32	42.99	13.75	2.95	7.99